

Figure 6. Pathogenic role of Treg cytotoxic transition to the orbital lesions of GO

(A) Schematic diagram of the EGFP labeled autoreactive Treg adoptive transfer experiment.

(B) The proportion of EGFP+ KLRC1+ cells within CD4+ cells in the peripheral blood of Healthy and GO mice after adoptive transfer experiment, representing the cytotoxic transition of Tregs in vivo (Healthy, n=3; GO, n=9). Data are represented as the median [IQR]. \*P < 0.05 by Mann-Whitney U test.

(C) Immunofluorescence staining demonstrated the presence of KLRC1+ EGFP+ cells in the orbital tissues of GO model mice.

(D, E) The major subtypes of orbital tissues (D) and integrated CD4 T cells from PBMCs and tissues (E) based on scRNA-seq data of Healthy donors and GO patients; the upper-right UMAP plot illustrates the batch effects.

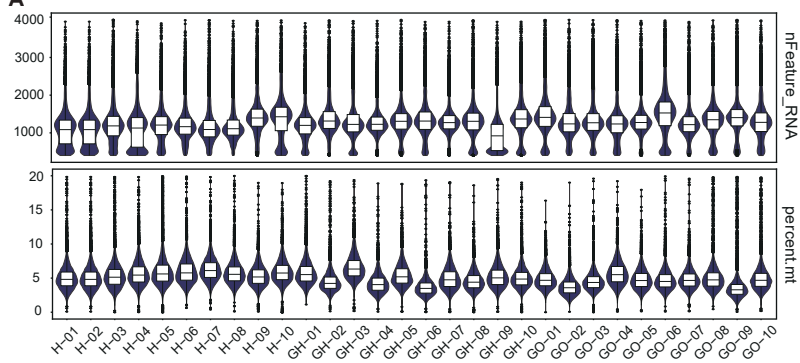
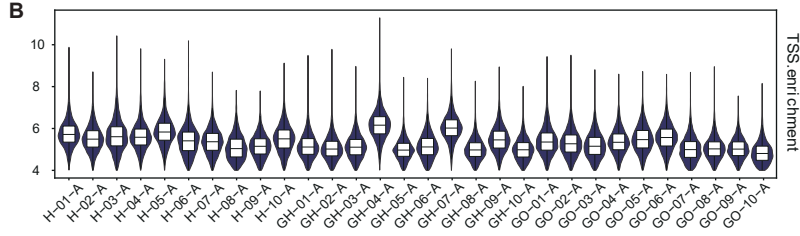
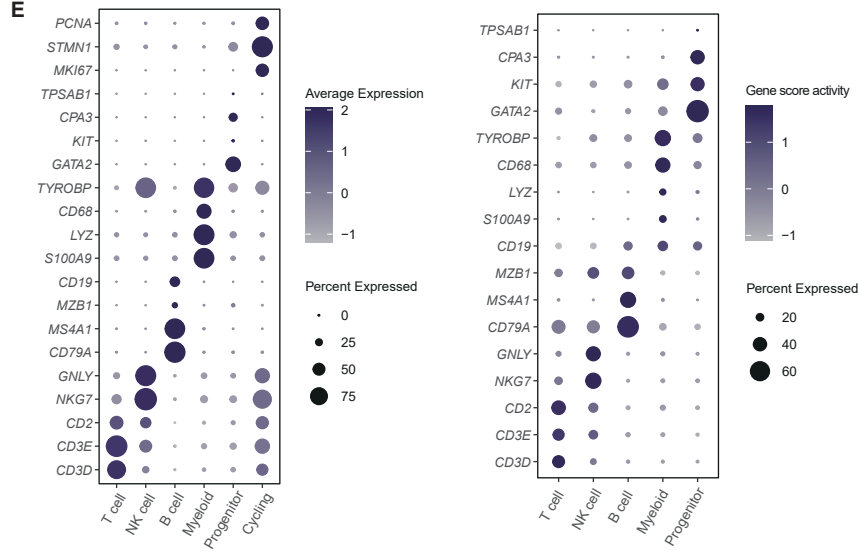
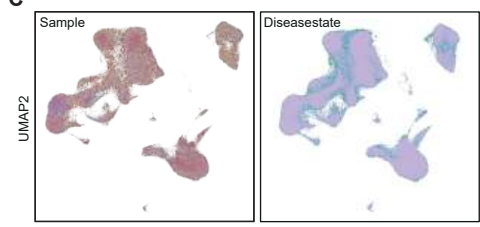
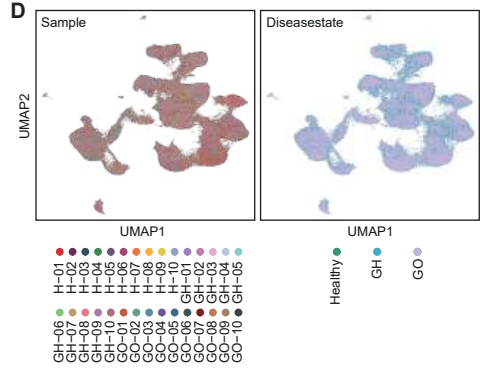
(F) The ligand-receptor interactions involving CD4 CTLs significantly altered in GO among three LPF subgroups, MYF, and COF. Red represents inflammation-regulating ligand-receptor interactions, while green indicates ligand-receptor interactions related to extracellular matrix remodeling.

(G) Experimental model of the pathogenic effect of Treg cytotoxic transformation on localised lesions in the orbit.

(H) Immunofluorescence showed the expression of specific proteins of OF cells in the co-culture system of healthy control and GO model mouse groups; The histogram on the right represents the quantitative statistics of these proteins. Data are represented as the median [IQR]. \*\*P < 0.001 by Mann-Whitney U test.

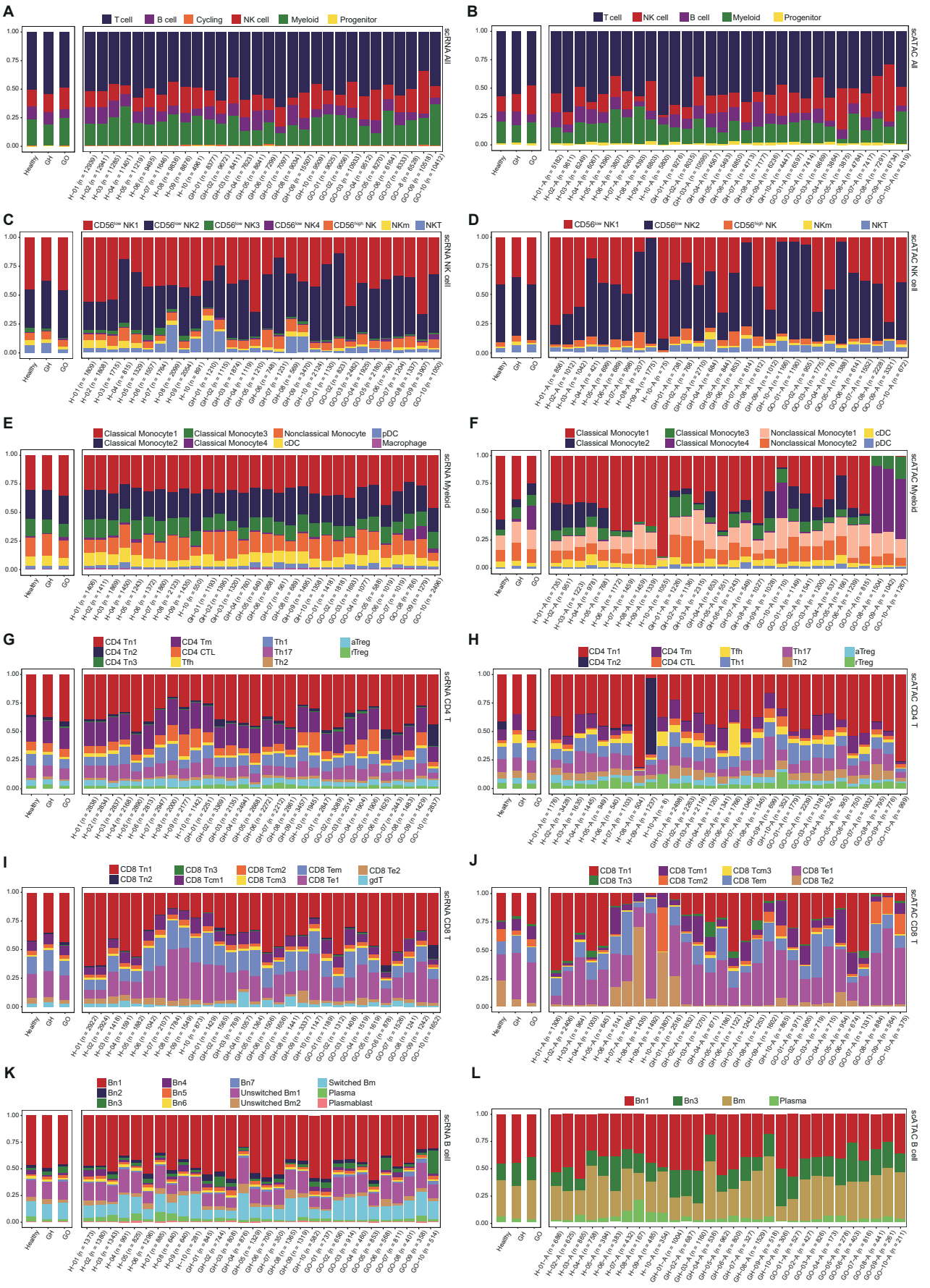
(I) qRT-PCR histogram showed the expression of specific genes in cells of the co-culture system. Each group consists of three independent samples (each n = 6). Data are represented as the median [IQR]. \*\*P < 0.001 by Mann-Whitney U test.

All experiments were repeated 3 times.

**A****B****E****C****D**

Supplemental Figure 1. Quality control and batch effect removal in single-cell datasets

- (A) Violin plots showed the distribution of the number of expressed genes and the percentage of mitochondrial RNA in each sample.
- (B) Violin plots depicted TSS enrichment in all cells of each sample, with the addition of "-A" for each identical sample suffix for easy differentiation with scRNA-seq.
- (C) UMAP representation of scRNA-seq after harmony correction on PCA dimensions, illustrating batch effects from sample batches, disease source batches.
- (D) UMAP representation of scATAC-seq after harmony correction on LSI dimensions, showing batch effects from sample batches, disease source batches, and gender batches.
- (E) Bubble plots of representative marker genes for all immune cell subtypes in the scRNA-seq and scATAC-seq datasets.





Supplemental Figure 2. Breakdown of cellular composition in the study samples

(A, B) Stacked bar plots showed the proportion of each major immune cell subtype in scRNA-seq (A) and scATAC (B) datasets for each sample. Each column represents a group (left) or a sample (right), with different colors indicating distinct cell types within the samples.

(C, D) Stacked bar plots illustrated the proportion of each NK cell subtype in scRNA-seq (C) and scATAC (D) datasets for each sample. Each column represents a group (left) or a sample (right), with different colors representing various cell types within the samples.

(E, F) Stacked bar plots displayed the proportion of each myeloid cell subtype in scRNA-seq (E) and scATAC (F) datasets for each sample. Each column represents a group (left) or a sample (right), with different colors indicating diverse cell types within the samples.

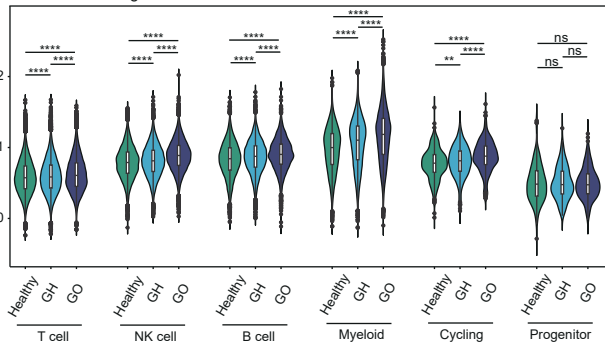
(G, H) Stacked bar plots indicated the proportion of each CD4 T cell subtype in scRNA-seq (G) and scATAC (H) datasets for each sample. Each column represents a group (left) or a sample (right), with different colors representing distinct cell types within the samples.

(I, J) Stacked bar plots represented the proportion of each CD8 T cell subtype in scRNA-seq (I) and scATAC (J) datasets for each sample. Each column represents a group (left) or a sample (right), with different colors indicating various cell types within the samples.

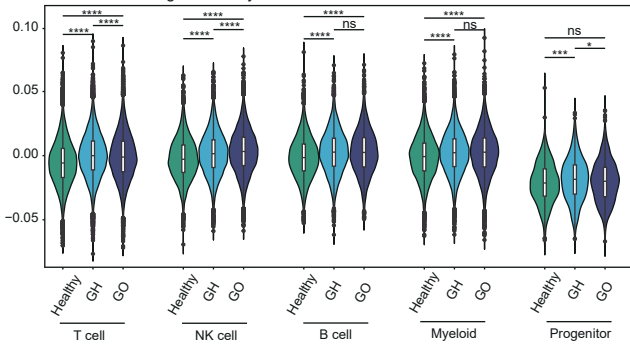
(K, L) Stacked bar plots depicted the proportion of each B cell subtype in scRNA-seq (K) and scATAC (L) datasets for each sample. Each column represents a group (left) or a sample (right), with different colors representing diverse cell types within the samples.

**A**

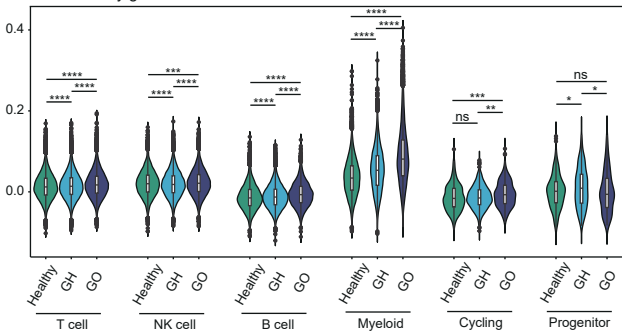
Graves' Disease gene score



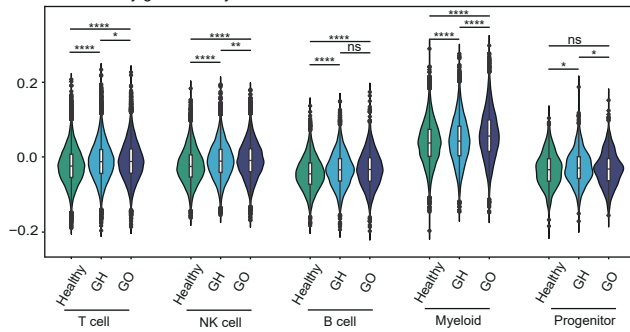
Graves' Disease gene activity score

**B**

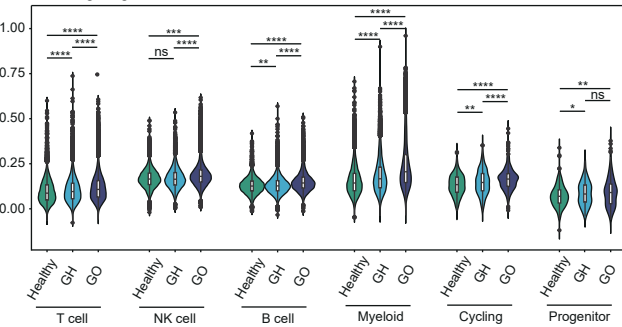
Inflammatory gene Score



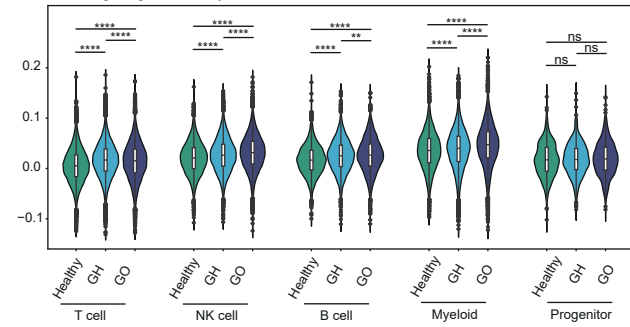
Inflammatory gene activity Score

**C**

IFNG signal gene Score



IFNG signal gene activity Score



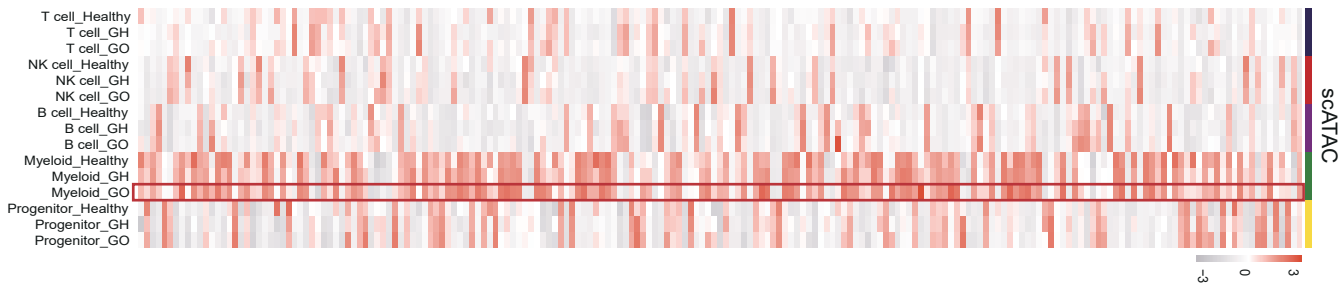
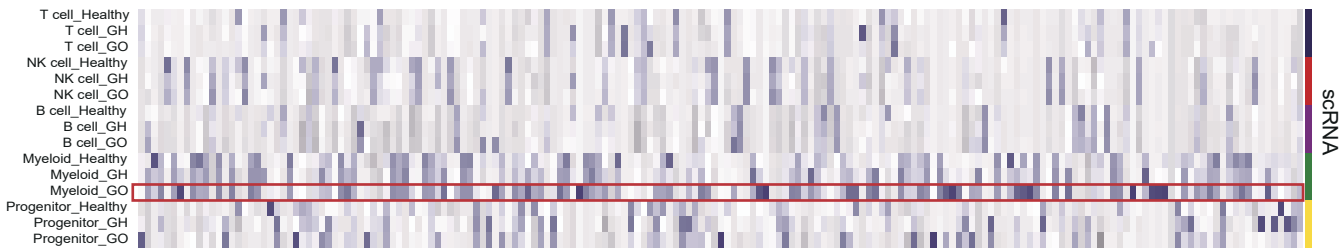
Supplemental Figure 3. Features of inflammatory immune environment within GO progression

(A) Violin plots displayed the gene expression and activity scores of the Graves' Disease gene set in major immune cell subtypes in the Healthy, GH, and GO groups. Data are represented as the median [IQR]. \*P.adj < 0.05, \*\*\*\*P.adj < 0.00001 by Mann-Whitney U test.

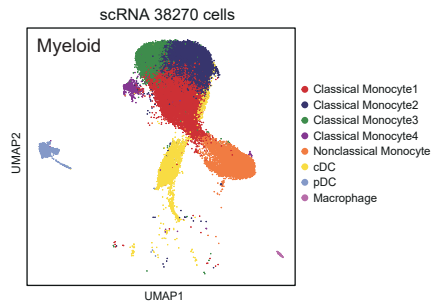
(B) Violin plots illustrated the gene expression and activity scores of the Inflammatory gene set in major immune cell subtypes in the Healthy, GH, and GO groups. Data are represented as the median [IQR]. \*P.adj < 0.05, \*\*\*\*P.adj < 0.00001 by Mann-Whitney U test.

(C) Violin plots presented the gene expression and activity scores of the IFNG signal gene set in major immune cell subtypes in the Healthy, GH, and GO groups. Data are represented as the median [IQR]. \*P.adj < 0.05, \*\*\*\*P.adj < 0.00001 by Mann-Whitney U test.

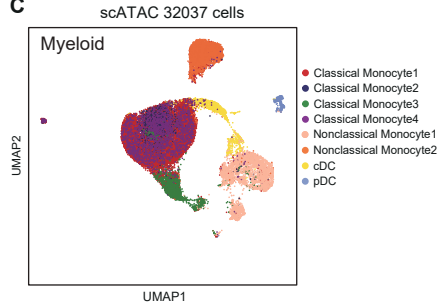
# Immflamation gene set



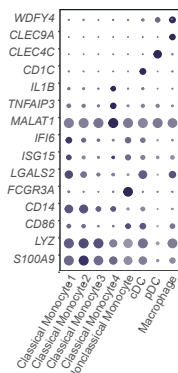
## B



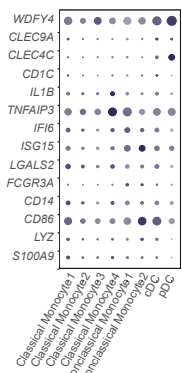
## C



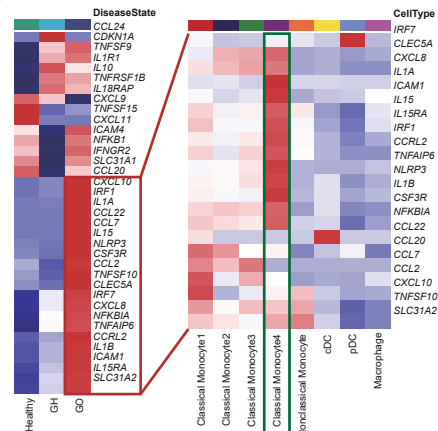
## D



## E



## F



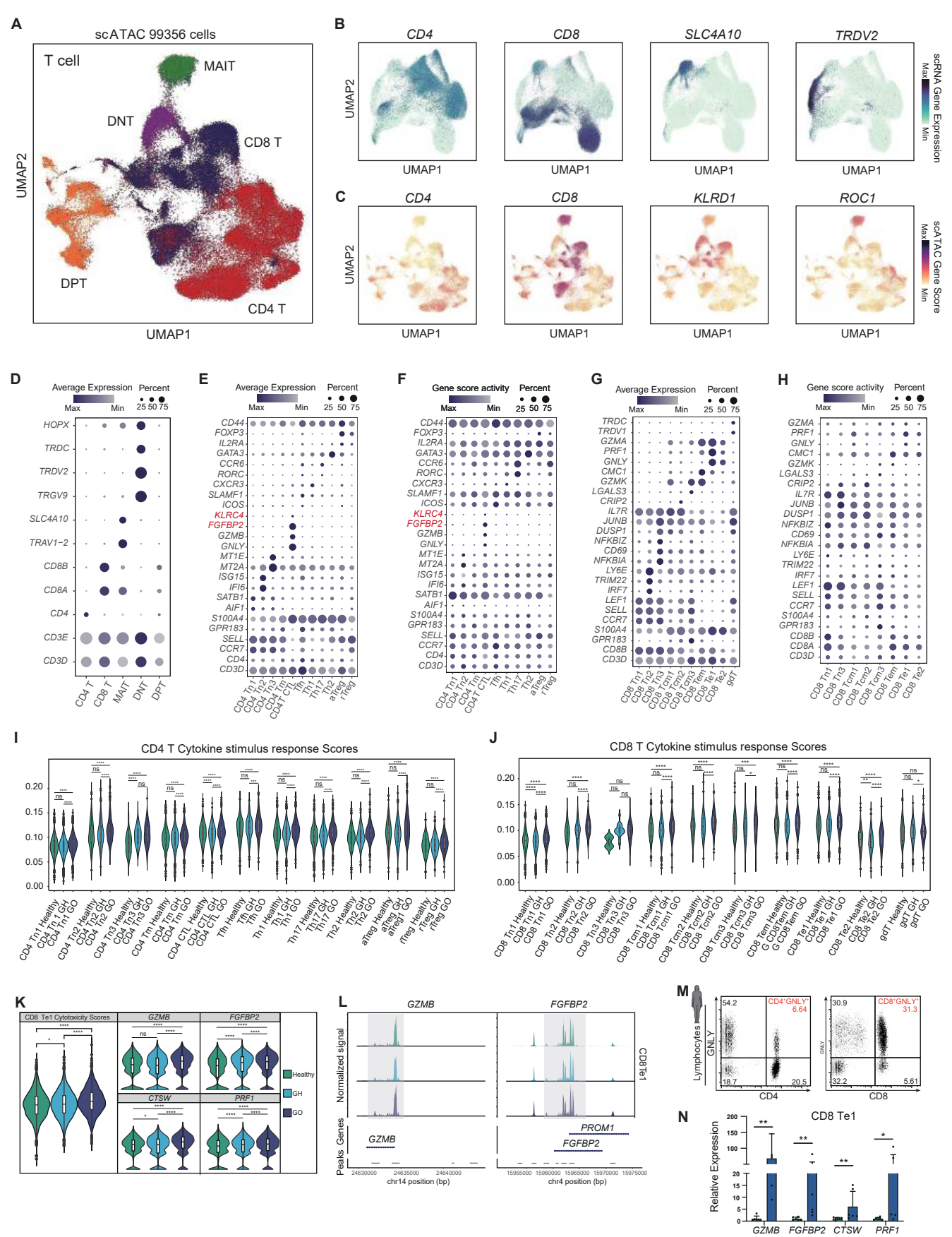
Supplemental Figure 4. Characterization of Myeloid subsets during GO progression

(A) Heatmaps illustrated the expression (up) and gene activity score (down) of Inflammation response gene (GSEA: M5932) among major cell types.

(B, C) UMAP plots depicted the clustering of all myeloid cell subtype in scRNA-seq (B) and scATAC-seq (C) datasets.

(D, E) Representative bubble plots of marker genes for each myeloid cell subtype in scRNA-seq (D) and scATAC-seq (E) datasets.

(F) Heatmap showed the expression levels of typical inflammatory genes in myeloid cells from Healthy, GH, and GO groups, as well as in each myeloid cell subtype.



Supplemental Figure 5. Annotation of T-cell subsets in single-cell datasets

(A) UMAP plot displayed the clustering of major T-cell subtypes in the scATAC-seq dataset.

(B, C) UMAP plots illustrated the expression levels (B) and gene activity scores (C) of typical marker genes for major T-cell subtypes.

(D) Bubble plot of representative marker genes for major T-cell subtypes in the scRNA-seq dataset.

(E, F) Bubble plots of representative marker genes for all CD4 T-cell subtypes in the scRNA-seq (E) and scATAC-seq (F) datasets.

(G, H) Bubble plots of representative marker genes for all CD8 T-cell subtypes in the scRNA-seq (G) and scATAC-seq (H) datasets.

(I, J) The expression scores of the CD4 T Cytokine stimulus response gene set in CD4 T-cell subtypes (I) and the CD8 T Cytokine stimulus response gene set in CD8 T-cell subtypes (J) from Healthy, GH, and GO groups. Data are represented as the median [IQR].

\*P.adj < 0.05, \*\*\*\*P.adj < 0.00001 by Mann-Whitney U test.

(K) The expression scores for the Cytotoxicity functional gene set and the gene expression levels of GZMB, FGFBP2, CTSW, and PRF1 in CD8 Te1 from Healthy, GH, and GO groups. Data are represented as the median [IQR]. \*P.adj < 0.05, \*\*\*\*P.adj < 0.00001 by Mann-Whitney U test.

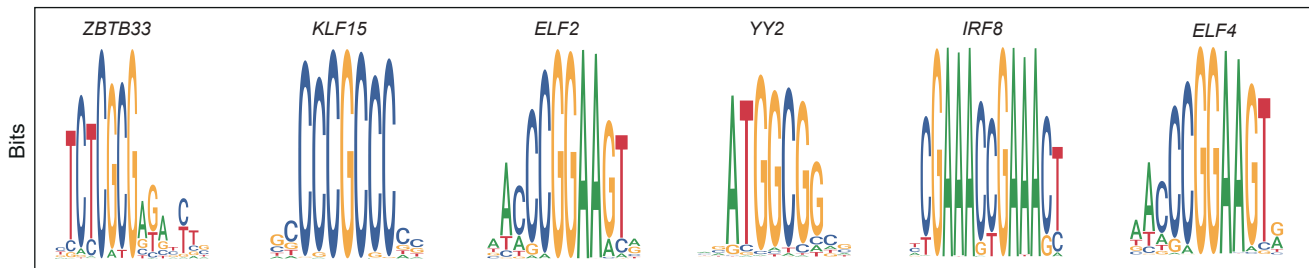
(L) Chromatin accessibility peak plots for GZMB and FGFBP2 genes in CD8 Te1 from Healthy, GH, and GO groups.

(M) Flow cytometry plots illustrated the sorting strategy for human PBMCs into CD4 CTL and GNLY+ CD8 T cells.

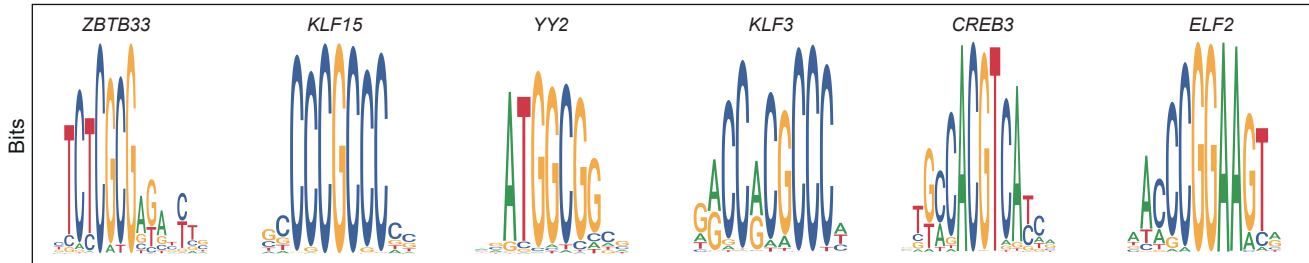
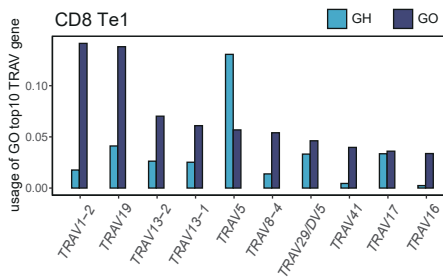
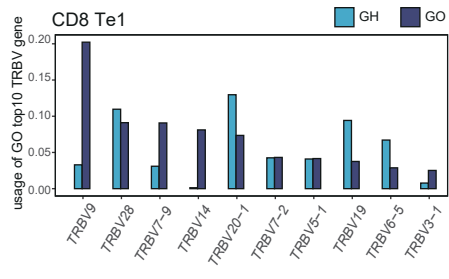
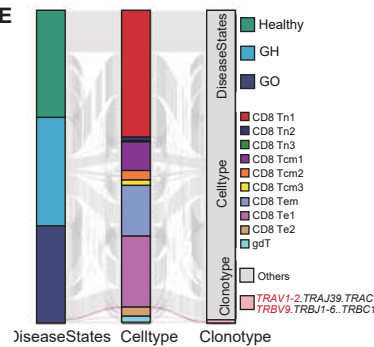
(N) Bar graphs from qRT-PCR showed the gene expression levels of GZMB, FGFBP2, CTSW, and PRF1 in CD8 Te1 from peripheral blood of Healthy and GO donors (Healthy, n=6; GO, n=6). Data are represented as the median [IQR]. \*P < 0.05, \*\*P < 0.001 by Mann-Whitney U test. The experiments were repeated 3 times.

**A**

## Top 6 Differential peaks motif of CD4 CTL

**B**

## Top 6 Differential peaks motif of CD8 Te1

**C****D****E**

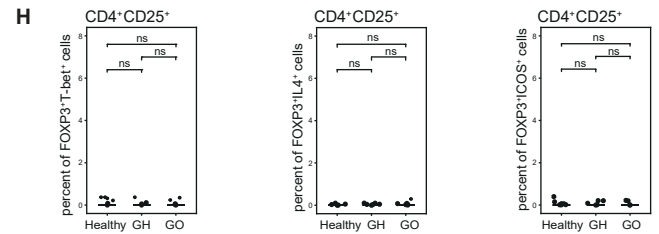
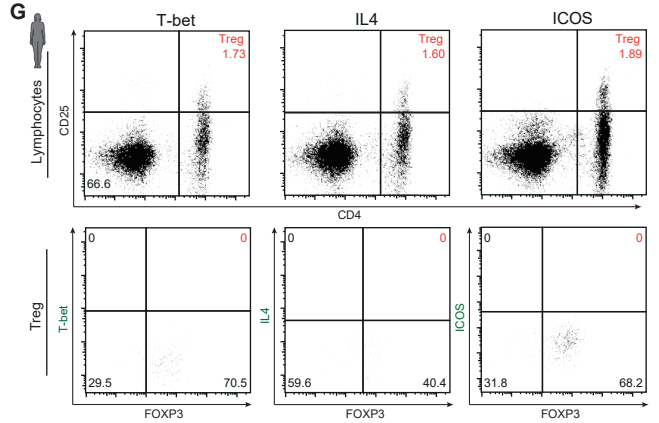
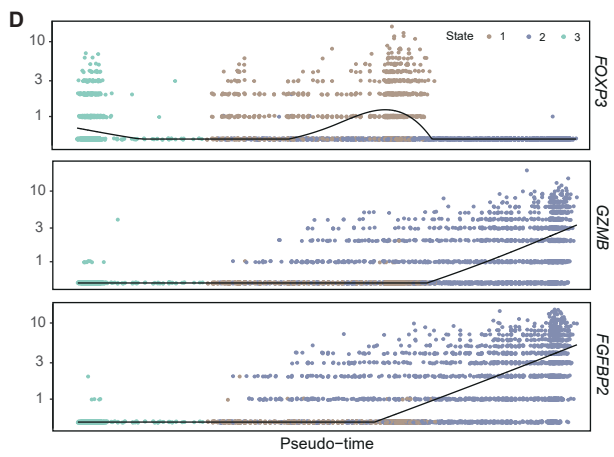
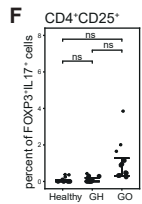
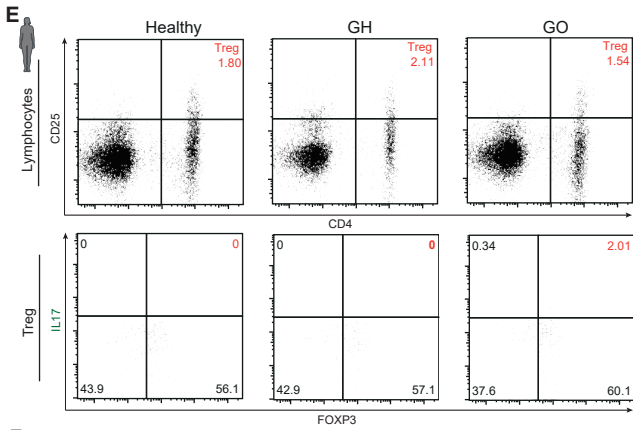
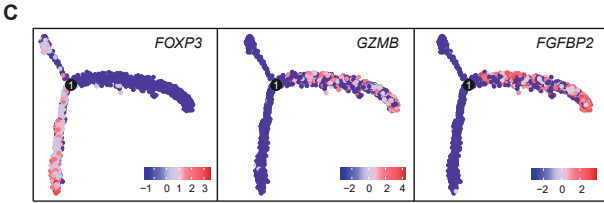
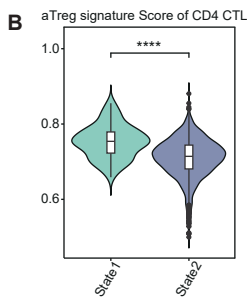
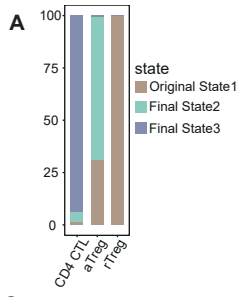


Supplemental Figure 6. Analysis of GO-specific TF and antigen clone epitopes

(A, B) Top 6 differential peaks motif analysis of in CD4 CTL (A) and CD8 Te1 (B) cells between GH and GO groups.

(C, D) Bar charts illustrated the expression levels of the top 10 GO-specific TRAV genes (G) and top 10 TRBV genes (H) in CD8 T-cell subtypes from Healthy, GH, and GO groups.

(E) Sankey diagram represented the relationship between clonotype genes in CD8 T-cell subtypes from Healthy, GH, and GO groups. GO-specific TCR are highlighted



Supplemental Figure 7. Detailed analysis of Treg during GO progression

(A) Stacked bar charts illustrated the proportions of CD4 CTL, aTreg, and rTreg at different time points.

(B) Violin plots depicted the expression scores of transcriptionally characteristic genes for aTreg in CD4 CTL from State1 and State2.

Data are represented as the median [IQR]. \*P.adj < 0.05, \*\*\*\*P.adj < 0.00001 by Mann-Whitney U test.

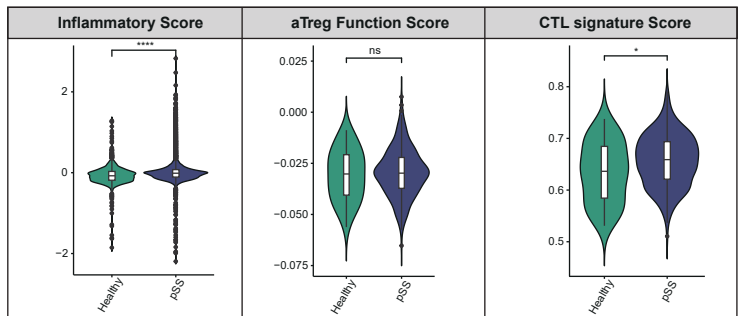
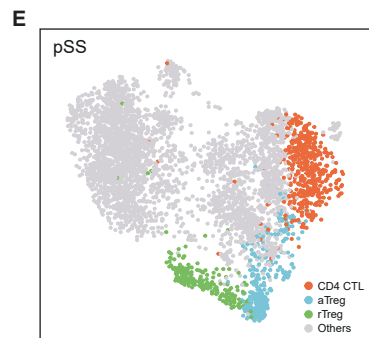
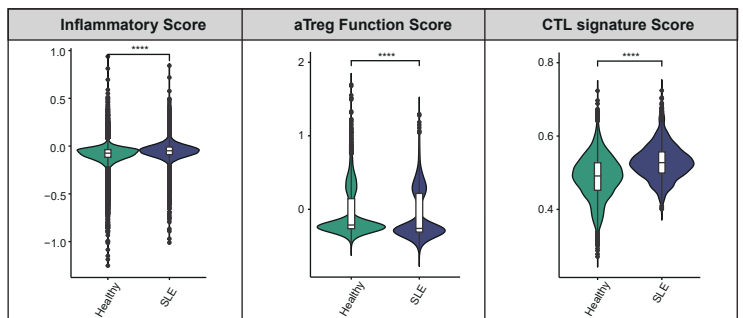
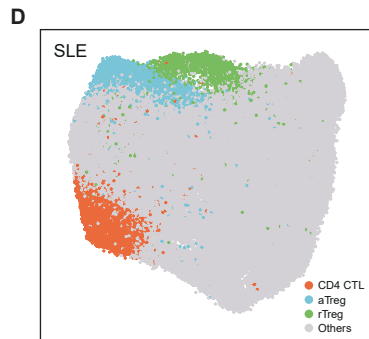
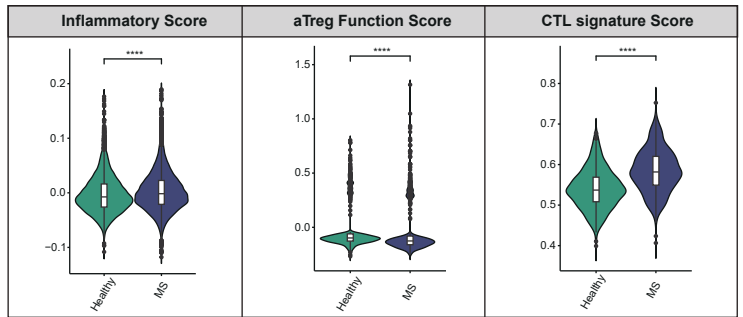
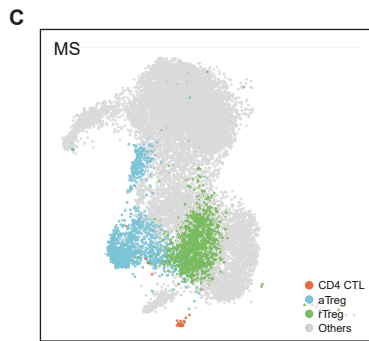
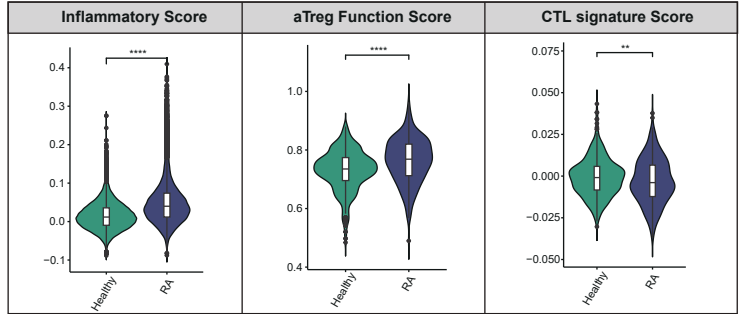
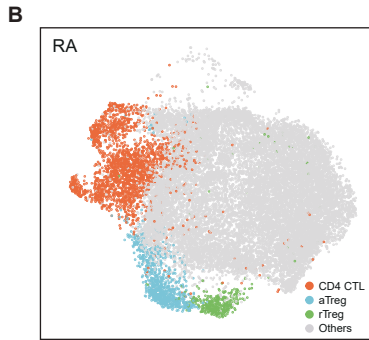
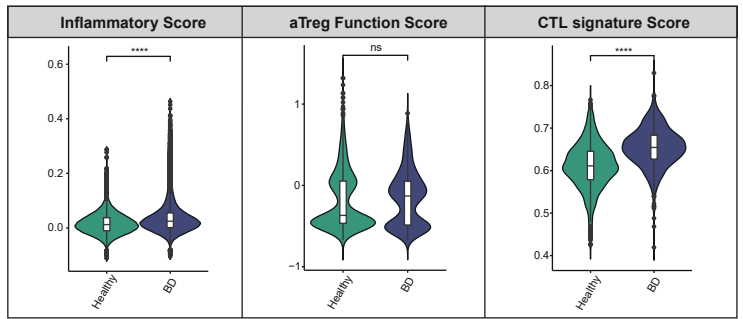
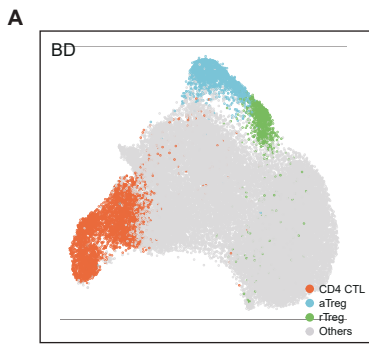
(C, D) Expression profiles of FOXP3, GZMB, and FGF2P2 genes across cells along a pseudotime trajectory.

(E, F) Flow cytometry plots and dot plots illustrated the expression of IL17 in CD4+ CD25+ FOXP3+ Treg from peripheral blood in Healthy, GH, and GO groups (Healthy, n=9; GH, n=9; GO, n=9). Data are represented as the median [IQR].

\*P.adj < 0.05 by Mann-Whitney U test.

(G, H) Flow cytometry plots and dot plots displayed the expression of T-bet, IL4, and ICOS in CD4+ CD25+ FOXP3+ Treg from the GO group in peripheral blood (Healthy, n=9; GH, n=9; GO, n=9). Data are represented as the median [IQR].

\*P.adj < 0.05 by Mann-Whitney U test.



Supplemental Figure 8. Observation of abnormal aTreg with elevated CTL transcriptional signature in other autoimmune diseases

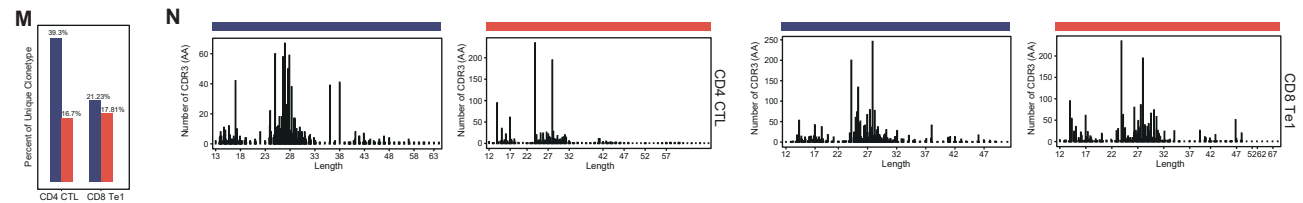
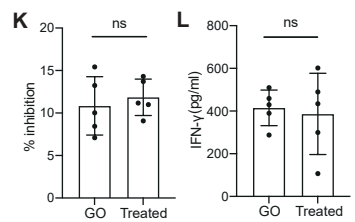
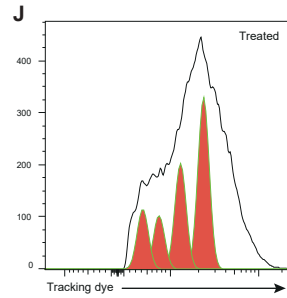
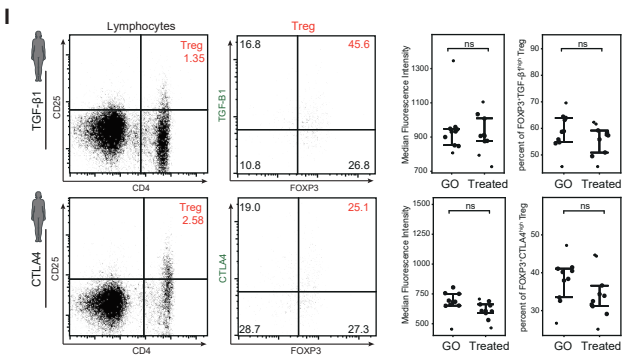
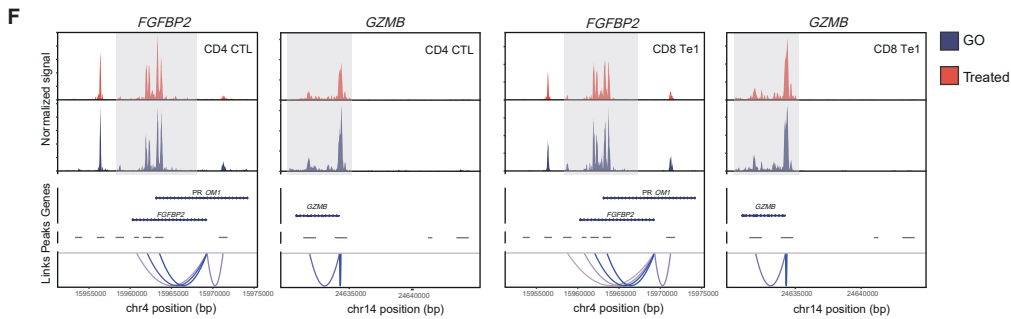
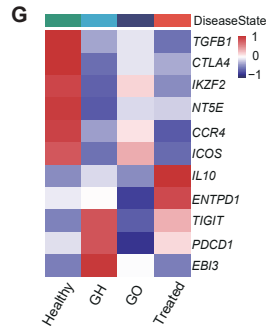
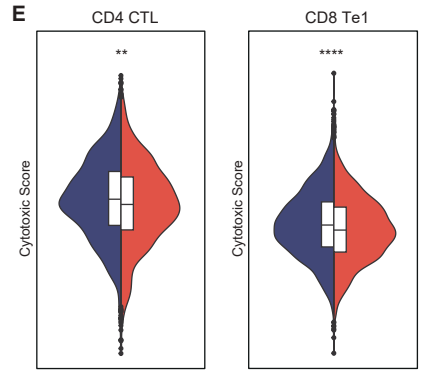
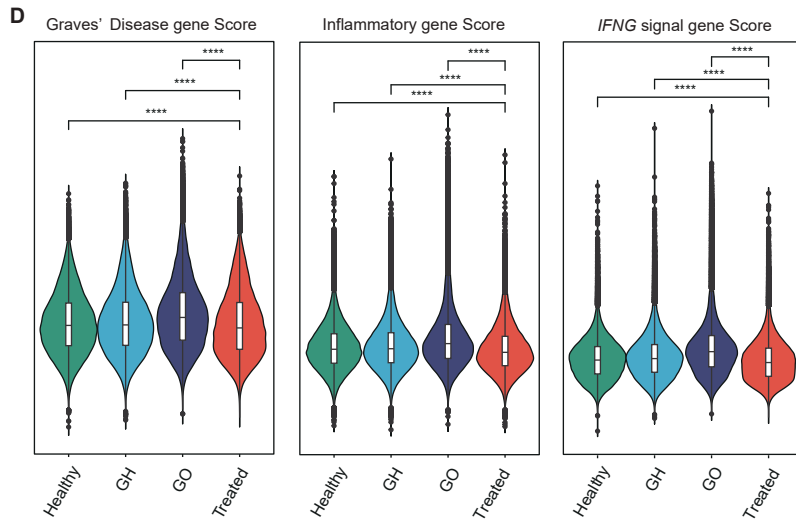
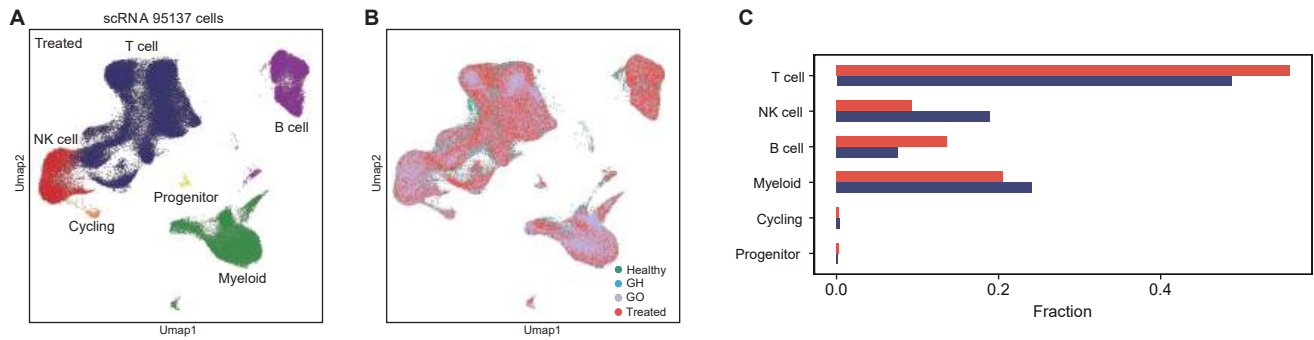
(A) Left: UMAP of CD4 CTL, aTreg, and rTreg in BD. Right: Violin plots depicting the overall inflammatory levels and the expression scores of the aTreg functional gene set and CD4 CTL transcriptional feature gene set in both healthy and BD groups. Data are represented as the median [IQR]. \*P.adj < 0.05, \*\*\*\*P.adj < 0.00001 by Mann-Whitney U test.

(B) Left: UMAP of CD4 CTL, aTreg, and rTreg in RA. Right: Violin plots displaying the overall inflammatory levels and the expression scores of the aTreg functional gene set and CD4 CTL transcriptional feature gene set in both healthy and RA groups. Data are represented as the median [IQR]. \*P.adj < 0.05, \*\*\*\*P.adj < 0.00001 by Mann-Whitney U test.

(C) Left: UMAP of CD4 CTL, aTreg, and rTreg in MS. Right: Violin plots presenting the overall inflammatory levels and the expression scores of the aTreg functional gene set and CD4 CTL transcriptional feature gene set in both healthy and MS groups. Data are represented as the median [IQR]. \*P.adj < 0.05, \*\*\*\*P.adj < 0.00001 by Mann-Whitney U test.

(D) Left: UMAP of CD4 CTL, aTreg, and rTreg in SLE. Right: Violin plots showing the overall inflammatory levels and the expression scores of the aTreg functional gene set and CD4 CTL transcriptional feature gene set in both healthy and SLE groups.

(E) Left: UMAP of CD4 CTL, aTreg, and rTreg in pSS. Right: Violin plots indicating the overall inflammatory levels and the expression scores of the aTreg functional gene set and CD4 CTL transcriptional feature gene set in both healthy and pSS groups. Data are represented as the median [IQR]. \*P.adj < 0.05, \*\*\*\*P.adj < 0.00001 by Mann-Whitney U test.



Supplemental Figure 9. Effects of corticosteroid therapy on patients with GO

(A) The distribution of major immune cell subtypes of the scRNA-seq dataset in Treated group.

(B) UMAP represented batch effects from four groups.

(C) The proportions of major immune cell subtypes.

(D) The expression scores of Graves' Disease, Inflammatory, and IFNG signal genes. Data are represented as the median [IQR].

\*\*\*\*P<sub>adj</sub> < 0.00001 by Mann-Whitney U test.

(E) The expression scores of cytotoxic genes in CD4 CTL and CD8 Te1 cells in the GO and Treated groups. Data are represented as the median [IQR]. \*\*\*\*P < 0.00001 by Mann-Whitney U test.

(F) Chromatin accessibility plots for FGFBP2 and GZMB genes in CD4 CTL and CD8 Te1 cells between the two groups.

(G) The expression levels of key treg's functional genes in aTreg.

(H) The aTreg function score of GO and Treated groups. Data are represented as the median [IQR]. \*P < 0.05 by Mann-Whitney U test.

(I) The expression levels and proportions of TGF- $\beta$ 1 and CTLA4 from human GO and Treated groups (GO, n=9; Treated, n=9). Data are represented as the median [IQR]. \*P < 0.05 by Mann-Whitney U test. The experiments were repeated 3 times.

(J) The proliferation of CD8+ T cells co-cultured with Treg cells of Treated group.

(K) The inhibition of CD8+ T cells co-cultured with Treg cells (GO, n=5; Treated, n=5). Data are represented as the median [IQR].

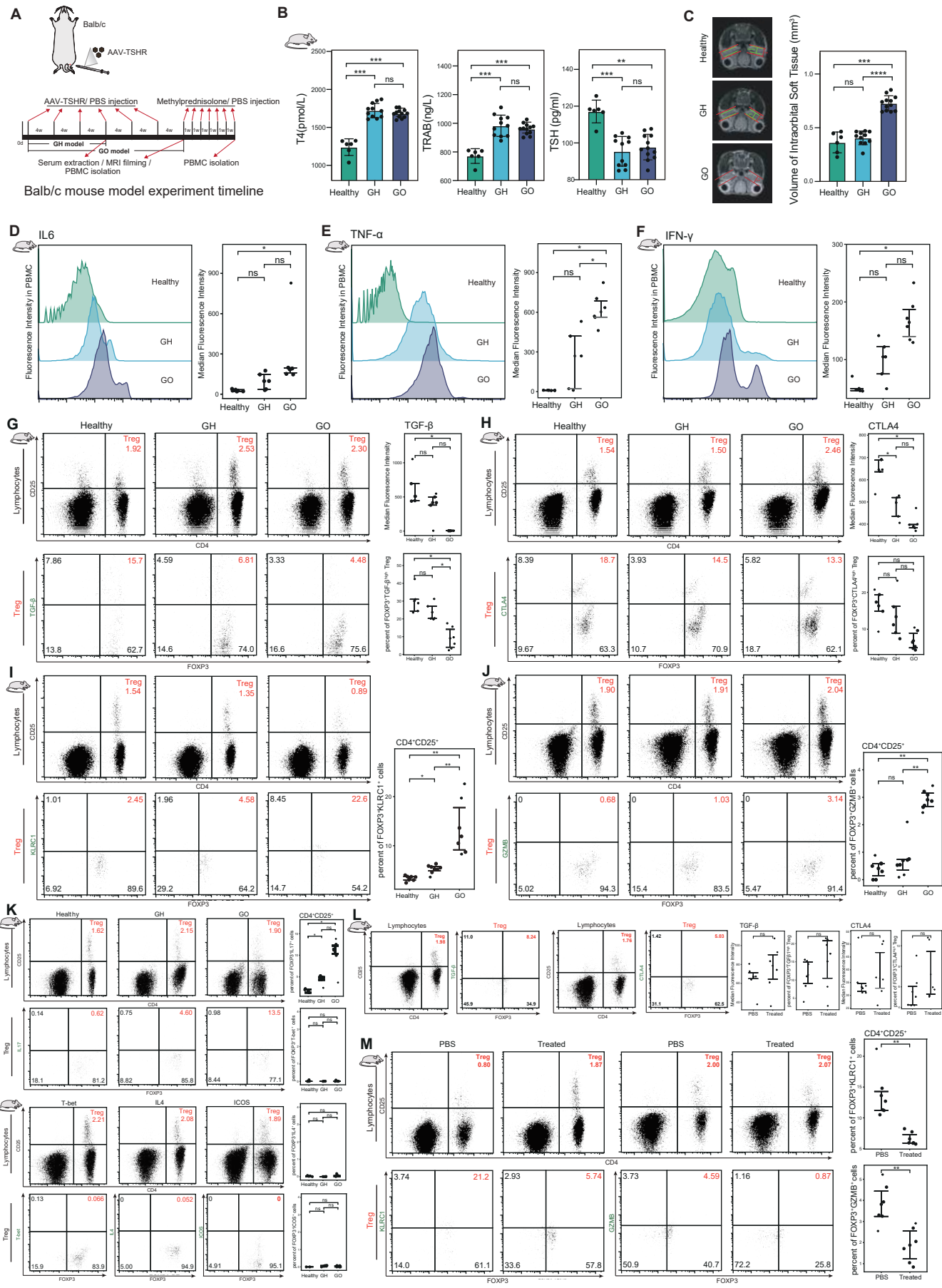
\*P < 0.05 by Mann-Whitney U test.

(L) The IFN- $\gamma$  production of CD8+ T cells co-cultured with Treg cells (GO, n=5; Treated, n=5). Data are represented as the median [IQR].

\*P < 0.05 by Mann-Whitney U test. The experiments were repeated 3 times.

(M) The unique clonal proportions of CD4 CTL and CD8 Te1 cells in the two groups.

(N) Composition of CD3 amino acids in CD4 CTL and CD8 Te1 in the two groups.





Supplemental Figure 10. Similarities of systemic inflammation and Treg characteristics between the GO mouse model and human GO patients

(A) The pipeline of the GO mouse model and the specific experimental time points.

(B, C) Criteria for determining the model in mouse: the expression of T4, TRAB and TSH (B), and the volume of orbital soft tissue (C) (Healthy, n=6; GH, n=11; GO, n=12). Data are represented as the median [IQR]. \*\*\*\*P.adj < 0.00001 by Mann-Whitney U test.

(D, E, F) The expression levels of IL6 (D), TNF- $\alpha$  (E), and IFN- $\gamma$  (F) of Healthy, GH, and GO mouse (Healthy, n=5; GH, n=5; GO, n=6). Data are represented as the median [IQR]. \*P.adj < 0.05 by Mann-Whitney U test.

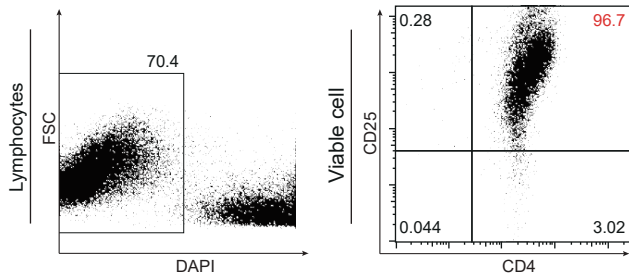
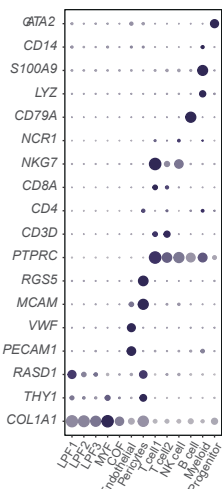
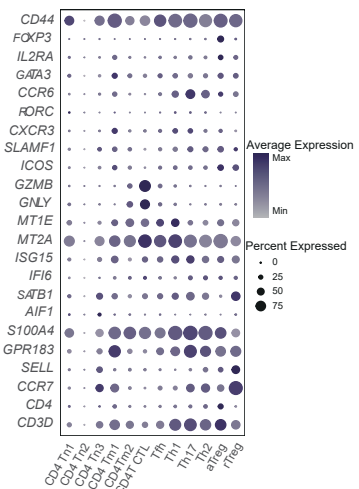
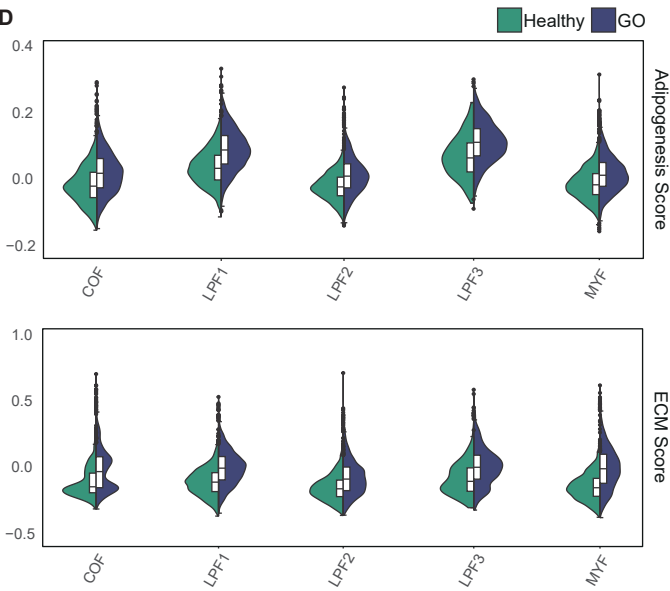
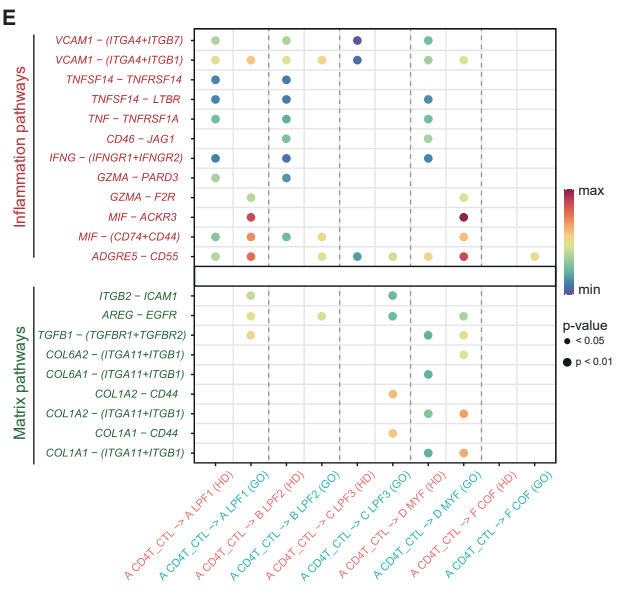
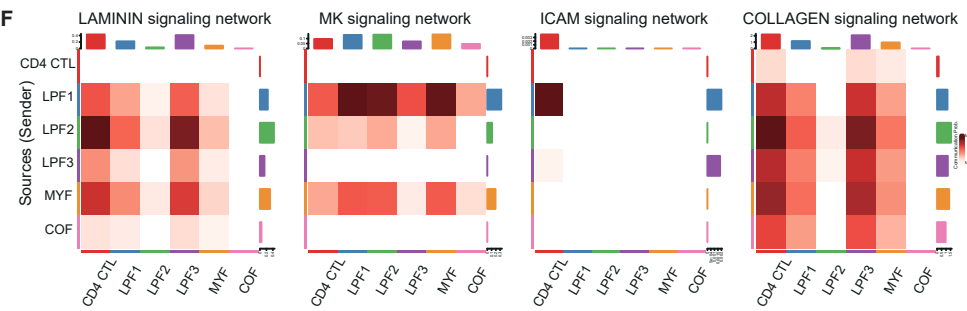
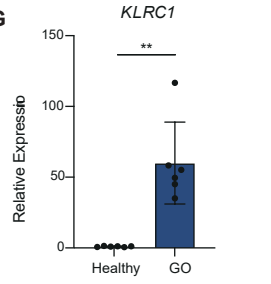
(G, H) The expression levels of TGF- $\beta$  (G) and CTLA4 (H) from three groups (Healthy, n=5; GH, n=5; GO, n=6). Data are represented as the median [IQR]. \*P.adj < 0.05 by Mann-Whitney U test.

(I, J) The expression levels of KLRC1 (I) and GZMB (J) from three groups (Healthy, n=7; GH, n=7; GO, n=7). Data are represented as the median [IQR]. \*P.adj < 0.05, \*\*P < 0.001 by Mann-Whitney U test.

(K) The expression levels of IL17 (top) and the expression levels of T-bet, IL4, and ICOS (bottom) from three groups (Healthy, n=5; GH, n=5; GO, n=6). Data are represented as the median [IQR]. \*P.adj < 0.05 by Mann-Whitney U test.

(L) The expression levels of TGF- $\beta$  and CTLA4 from GO and Treated groups (GO, n=6; Treated, n=6). Data are represented as the median [IQR]. \*P.adj < 0.05 by Mann-Whitney U test.

(M) The expression levels of KLRC1 and GZMB from GO and Treated groups (GO, n=6; Treated, n=6). Data are represented as the median [IQR]. \*\*P.adj < 0.001 by Mann-Whitney U test.

**A****B****C****D****E****F****G**

Supplemental Figure 11. Analysis related to orbital matrix remodeling in GO mouse model

(A) Flow cytometry plots displayed cell viability and the success rate of polarization of CD4+ T cells into Tregs in vitro.

(B) Bubble plot depicted characteristic markers of major subtypes in the orbital tissues of Healthy donors and GO patients.

(C) Bubble plot illustrated characteristic markers of integrated subtypes of CD4 T cells between orbital tissues and PBMC from Healthy donors and GO patients.

(D) Expression scores of Adipogenesis and ECM functional gene sets in all fibroblast subtypes of Healthy donors and GO patients.

(E) Differential signaling pathways between the Healthy and GO groups.

(F) Interaction strength of LAMININ, MK, ICAM, and COLLAGEN signaling network interactions between CD4 CTL and various fibroblast subtypes.

(G) The qRT-PCR bar chart displayed the expression of specific genes in Tregs after treatment with TSHR and TNF- $\alpha$ . Data are represented as the median [IQR]. \*\*P < 0.001 by Mann-Whitney U test. The experiments were repeated 3 times.